Low-Temperature Etching of Cu by Hydrogen-Based Plasmas

Fangyu Wu, Galit Levitin, and Dennis W. Hess*

School of Chemical and Biomolecular Engineering, Georgia Institute of Technology, 311 Ferst Drive, Atlanta, Georgia 30332-0100

ABSTRACT A simple, plasma-based, low-temperature etch process was developed for the subtractive etching of copper (Cu) films. Hydrogen (H_2) plasma etching of Cu thin films was performed in an inductively coupled plasma (ICP) reactor at temperatures below room temperature. This process achieved anisotropic Cu features and an etch rate of ~13 nm/min. Cu etch rate and patterning results were consistent with an etch process that involved both chemical and physical characteristics. This conclusion was reached by consideration of the plasma as a source of ultraviolet photons, ions, and hydrogen atoms, which promote Cu etching.

KEYWORDS: plasma • etching • Cu • low temperature • interconnects

The resistivity of interconnect materials is the primary determinant of integrated circuit (IC) speed for current and future devices (1, 2). Patterns are normally generated in these materials by plasma-assisted (subtractive) etching. However, because of the inability to form volatile Cu etch products during halogen-based plasma etching (3), damascene technology was introduced to avoid the need for Cu plasma etching (4). Although damascene technology played an essential role in the initial implementation of Cu metallization, a critical limitation has arisen because of the adherence of the IC industry to Moore's Law (5) and thus the reduction of minimum feature sizes. This limitation is the "size effect" of Cu, where the electrical resistivity of Cu increases rapidly as lateral dimensions are reduced below 100 nm, thereby approaching the electron mean free path in Cu (40 nm at 25 °C) (6−9).

Two approaches exist to reduce or eliminate the Cu size effect: decrease the Cu sidewall/surface roughness and grow larger Cu grains. However, grain growth of Cu in damascene technology is dramatically hindered by the narrow geometries (10) and impurities introduced into Cu that result from chemical mechanical planarization/polishing (CMP) and plating processes (11, 12). Therefore, development of new Cu patterning technologies that mitigate the size effect is required for future device generations. Subtractive etching may offer a viable approach. Indeed, etched tungsten (W) lines showed a distinctly lower resistivity than did W lines defined by the damascene process, where the resistivities reported were ~13 $\mu\Omega$-cm for plasma etched lines vs 18−23 $\mu\Omega$-cm for damascene lines (13). A similar advantage may therefore be expected for Cu.

Halogen-based (specifically chlorine-containing) plasmas have to date been the ones investigated to plasma etch Cu but removal of Cu etch products from the surface is hindered due to the relatively low volatility of Cu halides. Thus, high temperatures (>180 °C) have been generally invoked to enhance desorption of Cu chlorides (14−19). Alternatively, photon-enhanced removal of Cu chlorides at temperatures below 100 °C by laser (20), UV (21), or infrared radiation (22) has been reported. Both approaches introduce complexity and control issues into the patterning process. Cu halide product desorption has been averted by plasma chlorination or bromination of Cu followed by removal of the halides by immersion in dilute HCl solutions, thereby offering an alternative low temperature two-step approach to Cu patterning (23). Unfortunately, this method requires a combination of vacuum and liquid process and so increases the system complexity, reduces the manufacturing throughput, and may lead to process integration issues.

Recently, we developed a low temperature (10 °C) two-step Cu plasma etching process (24) based on a thermochemical analysis of solid−gas volatilization reactions in the Cu−Cl−H system (25). The Cu film is first chlorinated in a Cl_2 plasma to preferentially form $CuCl_2$ relative to CuCl (26). In the second step, a hydrogen plasma is used to convert $CuCl_2$ into a product with improved volatility, presumably Cu_3Cl_3 (27). Although this sequence represents an improvement relative to current approaches to plasma-based Cu etching, the process requires an etch sequence that will reduce overall etch rate and thus throughput. Our Cu patterning and etching mechanism studies for this two-step process indicated that the H_2 plasma treatment (2nd step) is rate-limiting and a critical component in establishing etch pattern fidelity (28). Thus in this report, we describe studies that demonstrate the ability to etch Cu films in a pure H_2 or H_2-based plasma at low temperatures. This surprising result offers a straightforward approach to patterning Cu using a simple plasma (vacuum) single-step process, thereby greatly improving manufacturability and process control.

Plasma etching of 100 nm Cu films was performed in an inductively coupled plasma (ICP) reactor. Figure 1a

* Corresponding author. E-mail: dennis.hess@chbe.gatech.edu.
Received for review April 9, 2010 and accepted July 12, 2010

DOI: 10.1021/am1003206

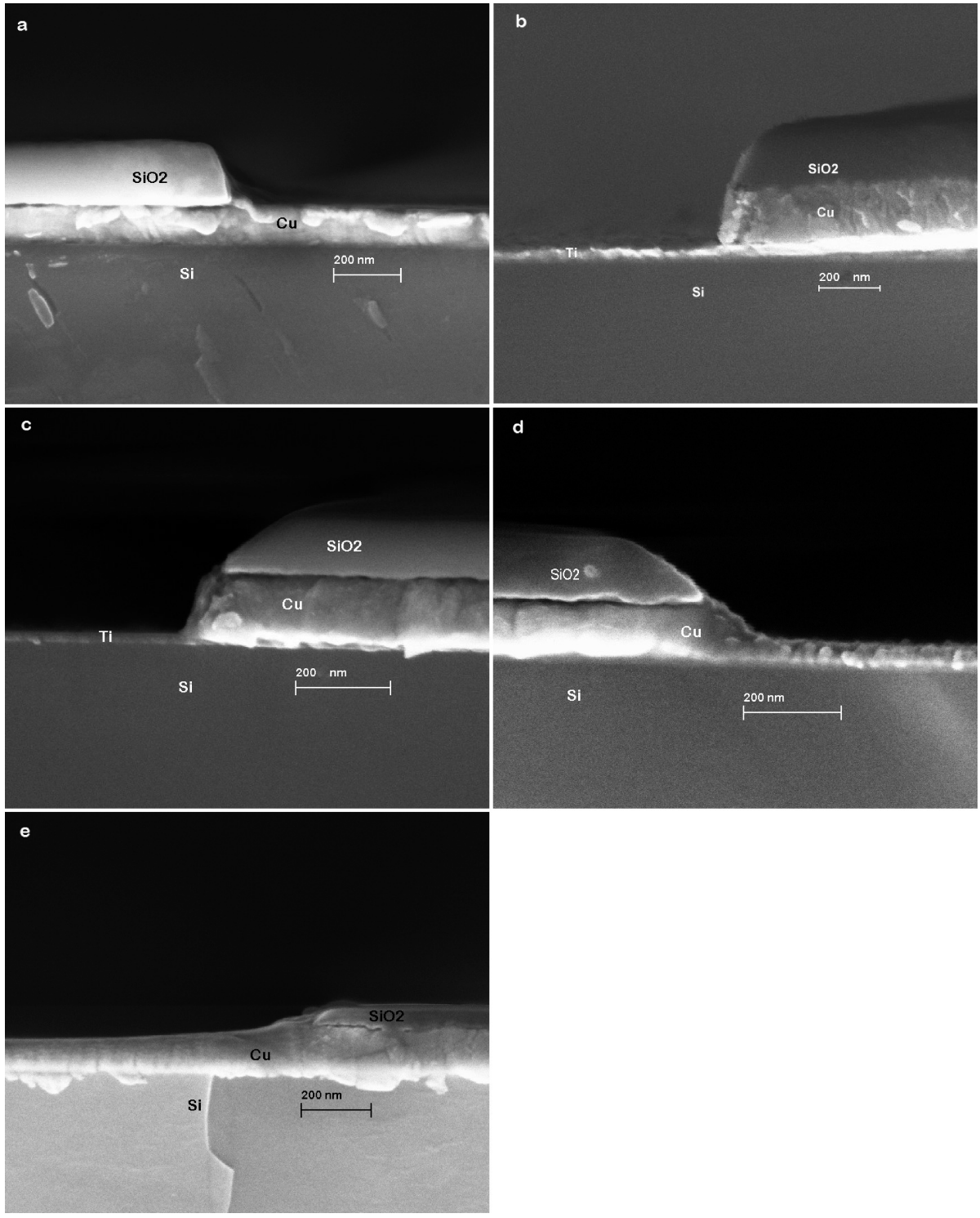

FIGURE 1. Cross-sectional SEMs of SiO_2 masked 100 nm Cu films. (a) After SiO_2 etching but prior to Cu etching; after 8 min plasma Cu etching with flows of (b) 50 sccm H_2, (c) 25 sccm H_2 + 25 sccm Ar, (d) 10 sccm H_2 + 40 sccm Ar, and (e) 50 sccm Ar. Other etch conditions were RF1 = 100 W, RF2 = 500 W, 20 mTorr pressure, and 10 °C electrode temperature.

shows a scanning electron microscope (SEM) image of an SiO_2-masked Cu film prior to etching; Figure 1b indicates that an 8 min H_2 plasma completely removed a 100 nm copper film (above a 20 nm Ti adhesion layer) under the conditions RF1 (platen power) = 100 W, RF2 (coil power) = 500 W, with flow rate and pressure 50 sccm and 20 mtorr, respectively. The temperature of the substrate electrode was assumed to be the same as that of the chiller (10 °C); clearly this is not the Cu surface temperature, but substantial temperature excursions (>20 °C) are unlikely over the etch time and conditions used. Figure 1b shows that etching terminated at the Ti adhesion layer, indicating that etch selectivity of Cu over Ti is possible. In addition, the Cu profile is anisotropic, although the sidewall surface is rough. This result demonstrates the feasibility of etching Cu with a pure H_2 plasma at low temperatures.

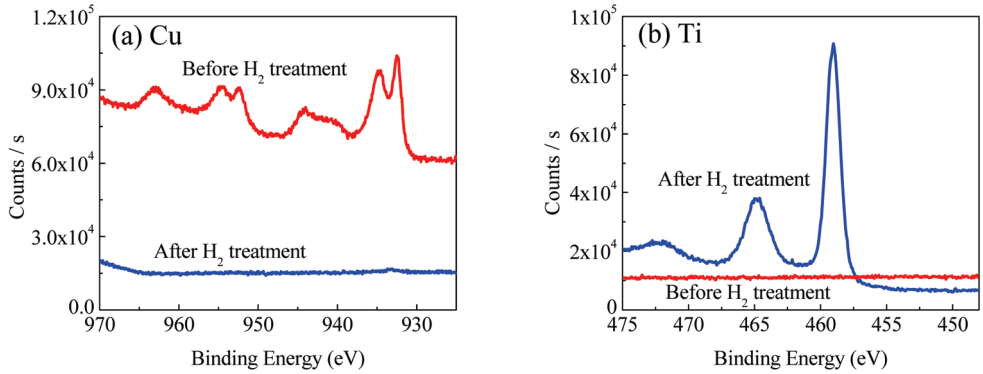

FIGURE 2. (a) Cu and (b) Ti 2p spectra (XPS) of 100 nm blanket Cu films before and after an 8 min (pure) H_2 plasma treatment. Atomic percentages of the surface before and after the H_2 treatment are Cu 2p, 15.92; O 1s, 35.81; C 1s, 48.26%; and Ti 2p, 16.47; O 1s, 48.12; C 1s, 28.31; F 1s, 2.91; N 1s, 4.18%, respectively. The carbon and oxygen detected are from exposure of the surfaces to air after etching. The small amount of F on the Ti surface after H_2 etch arose from the reactor chamber where a fluorine-based plasma is used to etch the SiO_2 mask in patterning studies.

Etch studies on blanket Cu samples were performed to gain additional insight into this H_2 plasma etching process. X-ray photoelectron spectroscopy (XPS) was used to probe blanket Cu surfaces before and after an 8 min H_2 etch cycle. Figure 2 shows that the untreated sample displays four characteristic peaks for Cu, but Ti is not detected since the sampling depth of XPS is <10 nm; after the H_2 plasma treatment, Cu peaks are not apparent which indicates removal of the Cu film by the H_2 plasma at least to the detectability limit of XPS. The appearance of Ti peaks after the etch process indicates that a H_2 plasma does not substantially etch Ti under these etch conditions.

This result is unexpected because copper hydrides are not predicted to have significant volatility (this issue is discussed in the following paragraphs), and H_2 should not efficiently sputter Cu because of the low molecular (or atomic) weight. We also note that the same H_2 etching capability was observed on electroplated Cu samples (145 nm electroplated Cu on 80 nm physical vapor deposited seed layer), which indicates that this phenomenon is not unique to e-beam evaporated Cu films. To gain additional insight into the role of ion bombardment in this Cu plasma etching process, argon was used as a Cu etchant to allow comparison of this more efficient sputter gas to results obtained with H_2.

Images c and e in Figure 1 are cross-sectional images of a 100 nm Cu film etched for 8 min in a 1:1 H_2:Ar plasma and in an Ar plasma, respectively. Both etch runs were performed with RF1 = 100 W, RF2 = 500 W, 20 mTorr pressure, and an electrode chiller temperature of 10 °C. The gas flows were: 50 sccm Ar for Ar plasma, 25 sccm H_2 plus 25 sccm Ar for H_2/Ar plasma. Figure 1e demonstrates that under these conditions, Ar is able to etch Cu, albeit at a low rate of <4 nm/min; this represents a pure sputter rate for Cu. However, significant ablation of the SiO_2 mask is apparent, consistent with the ability of Ar ion bombardment to remove materials by momentum transfer. However, the H_2/Ar plasma (Figure 1c) displays a much improved etch result compared to Ar (Figure 1e) and an improvement relative to that of a pure H_2 plasma (Figure 1b), with a smoother etched surface and higher etch rate (~ 16 nm/min under the conditions used). These results indicate that the mechanism involved in the H_2 plasma etching of Cu has a chemical component. The fact that directional etching with no discernible undercutting of the SiO_2 mask is observed in a H_2 plasma suggests that a physical (sputtering) component due to ion bombardment is also involved.

Because Ar ion bombardment should assist in the removal of Cu etch products due to the high atomic weight and thus momentum transfer, the effect of different H_2/Ar plasma mixtures was investigated. Figure 1b–e shows cross-sectional SEM images of masked Cu samples after 8 min of etching using different H_2: Ar ratios. Clearly, the etch profile anisotropy degrades with increasing Ar concentration. Also, the etch rate of Cu relative to SiO_2 increases and then decreases as the Ar concentration increases. Specifically, the etch rates for these different ratios were 13, 16, 10, and 4 nm/min, respectively, which indicates that an optimum combination of chemical and physical effects exists for efficient Cu etching. Enhanced ion bombardment assists desorption, but the presence of hydrogen, probably H, is critical to effective etching. Finally, the increased sidewall slope that results from increasing Ar concentration (Figures 1b–e) is consistent with increased sputter rate of the SiO_2 mask which yields sloped sidewalls (29). These results confirm our conclusion regarding the importance of a chemical component in the plasma-assisted etching of Cu in H_2-based plasmas.

Preliminary effects of temperature changes were also investigated by increasing the substrate temperature from 10 to 40 °C in 15° increments. H_2 plasma etch conditions were the same as those of previous etch studies, although 300 nm thick Cu samples were used to allow etch depths to be measured by profilometry and thereby obtain etch rates. Over this small temperature regime, etch rates were not affected by temperature; etch rates for all experiments were ~13 nm/min. Because of equipment limitations, higher temperatures were not possible with this reactor system; further studies are underway using other plasma reactors. These observations indicate that at least over the narrow range of temperatures investigated, H_2 plasma-based etching of Cu films offers a wide temperature control window for implementation of a manufacturable etch process. Possible

reasons for the volatilization of Cu in these low-temperature processes are discussed in the following paragraphs.

Hydrogen, especially in the atomic form, has a high chemical reactivity and lattice mobility; indeed, H embrittlement of Cu is an important source of Cu degradation (30). In a plasma environment, H^+ or $H^\bullet$ can react with film material and release H into the solid, which can cause the formation of defects or highly metastable phases (31). Introduction of hydrogen into fcc metals has resulted in microstructure changes; specifically with copper, microbubbles may be generated (30). These observations suggest that Cu hydrides may form as a result of plasma exposure. However, thermodynamic calculations indicate that the vapor pressures of Cu hydrides (CuH, CuH_2, or other CuH_x species) are too low to substantially enhance vapor phase Cu removal or etching (25). Because we observed that the Cu etch rate in a pure H_2 plasma was higher than that for the two-step etch process (chlorination followed by hydrogen treatment) (28), alternate mechanisms for Cu etch product desorption must be considered.

In a H_2 plasma, the Cu surface is bombarded by ions and electrons, as well as UV and visible photons; these particles and photons supply energy to the Cu surface and can enhance etch product removal. Indeed, photodesorption of metal atoms have been reported upon exposure of alkali metals such as Na, K, and Cs to photons (32); specifically, desorption of sodium atoms was detected even with 40 mW/cm^2 cw laser exposure, where the excitation wavelength was 514 nm (33). As indicated by the atomic spectrum of hydrogen (34), intense atomic lines in the UV wavelength range of 90−120 nm will be present in the H_2 plasma. Although CuH is reported to be thermally unstable, even at 0 °C (35), more recent studies suggest that in the presence of a high hydrogen pressure or high hydrogen activity, CuH might be formed (36). It is also likely that this reaction may be promoted by the presence of H (e.g., from the plasma atmosphere) which can react with Cu. If sufficient stability of CuH is achieved, desorption of this product may be enhanced by ion and/or photon bombardment. Therefore, photon-assisted desorption of products such as CuH may be important in Cu removal using H_2 plasmas.

These observations are consistent with reports of photon-enhanced removal of copper chloride etch products using UV (21) or even IR radiation (22). In these studies, UV radiation was believed to promote the surface reaction between Cu and chlorine by lowering the activation energy of Cu to preferentially form specific Cu chlorides (CuCl or $CuCl_2$). However, our studies (28) as well as those of previous investigators (26), have demonstrated that Cu chlorination occurs rapidly and thus should not limit Cu removal rates. Thus, the enhanced etch rates of Cu in chlorine plasmas due to photon irradiation as demonstrated in previous studies may have resulted from photon assisted etch product removal rather than from reaction rate enhancement. Such observations combined with the high energy photon emission that occurs in H_2 plasmas (34) and the reduced removal rates with Ar which is known to be an effective sputter gas, suggest that UV enhanced desorption of Cu etch products in a H_2 plasma is plausible; studies to investigate this possibility are underway.

The surprising results in this study showed that thin Cu films (blanket and SiO_2 masked) were etched in a H_2 plasma at temperatures below room temperature, with an anisotropic profile and high selectivity over Ti. Etch rate variation of pure Ar and H_2/Ar plasmas indicated that chemical and physical components were involved in the etch process. Although the etch mechanism is not yet understood, these preliminary studies suggested that chemical effects and ion bombardment play a role in the low-temperature H_2-based Cu etch process, and photon enhancement may be involved as well.

EXPERIMENTAL METHODS

Copper films of 100 or 300 nm thickness were deposited by e-beam evaporation (CVC E-Beam Evaporator) onto silicon wafers that had been coated with 20 nm of titanium to promote Cu adhesion to silicon. Electroplated Cu films (145 nm electroplated Cu films grown from an 80 nm physical vapor deposited (PVD) seed layer followed by annealing at 200 °C in forming gas for 30 s) were also studied. Because no differences in etch properties were observed, the results reported in this paper are from e-beam deposited Cu films. Cu-coated substrates were sectioned into etch samples ~1 cm^2. Plasma etching of thin Cu films was performed in an inductively coupled plasma (ICP) reactor (Plasma Therm ICP). The substrate temperature was maintained at ~10 °C using a water cooled chiller connected to the substrate electrode. The H_2 gas flow rate was 50 standard cubic centimeters per minute (sccm) and the reactor pressure was maintained at 20 mtorr. The radio frequency power applied to the ICP coil (RF2) was 500 W, whereas the power applied to the substrate (RF1) was 100W. Both blanket and masked Cu films were investigated in these plasma etch atmospheres. Masked Cu films invoked SiO_2 (~150 nm) as the mask layer. The SiO_2 film was deposited in a Plasma Therm PECVD (plasma enhanced chemical vapor deposition) system with 400 sccm SiH_4 and 900 sccm N_2O as precursors; the substrate electrode was heated to 250 °C, the power applied to the electrode was 25 W, and the pressure was maintained at 900 mtorr during the deposition process. Mask patterns were generated by fluorine-based plasma etching within the same ICP reactor: the etch gas was a mixture of 25 sccm Ar, 2 sccm O_2, 14 sccm CF_4, and 6 sccm C_4F_6, RF1 was 200 W and RF2 was 100 W, whereas the process pressure was maintained at 5 mTorr. Chemical analysis of the films and surfaces before and after plasma etching was performed using X-ray photoelectron spectroscopy (XPS). XPS spectra were collected using a Thermo Scientific K-Alpha XPS. Cu film patterns were examined with a scanning electron microscope (SEM, Zeiss SEM Ultra60). Thickness changes of the Cu layer were determined from SEM images and a Wyko Profilometer.

Acknowledgment. The authors thank Dr. Kevin Martin, Gary Spinner, and other clean room staff members in the

Microelectronics Research Center (MiRC) at the Georgia Institute of Technology for assistance with the ICP reactor. This work was supported by the National Science Foundation under Grant CBET 0755607.

REFERENCES AND NOTES

(1) Bohr, M. T. *Solid State Technol.* **1996**, *39*, 105–108.
(2) Bohr, M. T.; El-Mansy, Y. A. *IEEE Trans. Electron Devices* **1998**, *45*, 620–625.
(3) Steinbruchel, C. *Appl. Surf. Sci.* **1995**, *91*, 139–146.
(4) Edelstein, D.; Heidenreich, J.; Goldblatt, R.; Cote, W.; Uzoh, C.; Lustig, N.; Roper, P.; McDevitt, T.; Motsiff, W.; Simon, A.; Dukovic, J.; Wachnik, R.; Rathore, H.; Schulz, R.; Su, L.; Luce, S.; Slattery, J. *Tech. Dig.—Int. Electron Devices Meet.* **1997**, 773–776.
(5) Moore, G. E. *Electronics* **1965**, 114–117.
(6) Mallikarjunan, A.; Sharma, S.; Murarka, S. P. *Electrochem. Solid-State Lett.* **2000**, *3*, 437–438.
(7) Liu, H. D.; Zhao, Y. P.; Ramanath, G.; Murarka, S. P.; Wang, G. C. *Thin Solid Films* **2001**, *384*, 151–156.
(8) Steinhogl, W.; Schindler, G.; Steinlesberger, G.; Traving, M.; Engelhardt, M. *J. Appl. Phys.* **2005**, *97*, 023706—1-7.
(9) Steinhoegl, W.; Schindler, G.; Engelhardt, M. *Semiconductor Int.* **2005**, *28*, 34–38.
(10) Wu, W.; Ernur, D.; Brongersma, S. H.; Van Hove, M.; Maex, K. *Microelectron. Eng.* **2004**, *76*, 190–194.
(11) Zhang, W.; Brongersma, S. H.; Heylen, N.; Beyer, G.; Vandervorst, W.; Maex, K. *J. Electrochem. Soc.* **2005**, *152*, C832–C837.
(12) Vereecken, P. M.; Binstead, R. A.; Deligianni, H.; Andricacos, P. C. *IBM J. Res. Dev.* **2005**, *49*, 3–18.
(13) Traving, M.; Schindler, G.; Engelhardt, M. *J. Appl. Phys.* **2006**, *100*, 094325—4.
(14) Howard, B. J.; Steinbruchel, C. *J. Vac. Sci. Technol., A* **1994**, *12*, 1259–1264.
(15) Bertz, A.; Werner, T.; Hille, N.; Gessner, T. *Appl. Surf. Sci.* **1995**, *91*, 147–151.
(16) Lee, S. K.; Chun, S. S.; Hwang, C. Y.; Lee, W. J. *Jpn. J. Appl. Phys., Part 1* **1997**, *36*, 50–55.
(17) Nakakura, C. Y.; Altman, E. I. *Surf. Sci.* **1997**, *370*, 32–46.
(18) Lee, J. W.; Park, Y. D.; Childress, J. R.; Pearton, S. J.; Sharifi, F.; Ren, F. *J. Electrochem. Soc.* **1998**, *145*, 2585–2589.
(19) Armacost, M.; Hoh, P. D.; Wise, R.; Yan, W.; Brown, J. J.; Keller, J. H.; Kaplita, G. A.; Halle, S. D.; Muller, K. P.; Naeem, M. D.; Srinivasan, S.; Ng, H. Y.; Gutsche, M.; Gutmann, A.; Spuler, B. *IBM J. Res. Dev.* **1999**, *43*, 39–72.
(20) Tang, H.; Herman, I. P. *Appl. Phys. Lett.* **1992**, *60*, 2164–2166.
(21) Hahn, Y. B.; Pearton, S. J.; Cho, H.; Lee, K. P. *Mater. Sci. Eng., B* **2001**, *79*, 20–26.
(22) Ohshita, Y.; Hosoi, N. *Thin Solid Films* **1995**, *262*, 67–72.
(23) Kuo, Y.; Lee, S. *Appl. Phys. Lett.* **2001**, *78*, 1002–1004.
(24) Tamirisa, P. A.; Levitin, G.; Kulkarni, N. S.; Hess, D. W. *Microelectron. Eng.* **2007**, *84*, 105–108.
(25) Kulkarni, N. S.; DeHoff, R. T. *J. Electrochem. Soc.* **2002**, *149*, G620–G632.
(26) Sesselmann, W.; Chuang, T. J. *Surf. Sci.* **1986**, *176*, 32–66.
(27) Guido, M.; Balducci, G.; Gigli, G.; Spoliti, M. *J. Chem. Phys.* **1971**, *55*, 4566–4572.
(28) Wu, F.; Levitin, G.; Hess, D. W. *J. Electrochem. Soc.* **2010**, *157*, H474–H478.
(29) Chapman, B. *Glow Discharge Processes: Sputtering and Plasma Etching*; Wiley: New York, 1980.
(30) Zielinski, A. *Acta Metall. Mater.* **1990**, *38*, 2573–2582.
(31) Myers, S. M.; Baskes, M. I.; Birnbaum, H. K.; Corbett, J. W.; DeLeo, G. G.; Estreicher, S. K.; Haller, E. E.; Jena, P.; Johnson, N. M.; Kirchheim, R.; Pearton, S. J.; Stavola, M. J. *Rev. Mod. Phys.* **1992**, *64*, 559–617.
(32) Miller, J. C.; Haglund, R. F. In *Laser Ablation: Mechanisms and Applications: Proceedings of a Workshop*; Oak Ridge, TN, April 8—10, 1991; Springer-Verlag: Berlin, 1991; Vol. 389, pp 77—81.
(33) Hoheisel, W.; Jungmann, K.; Vollmer, M.; Weidenauer, R.; Träger, F. *Phys. Rev. Lett.* **1988**, *60*, 1649–1652.
(34) Candler, C. *Atomic Spectra and the Vector Model*, 2nd ed.; Van Nostrand: Princeton, NJ, 1964.
(35) Fitzsimons, N. P.; Jones, W.; Herley, P. J. *J. Chem. Soc., Faraday Trans.* **1995**, *91*, 713–718.
(36) Burtovyy, R.; Utzig, E.; Tkacz, M. *Thermochim. Acta* **2000**, *363*, 157–163.

AM1003206